Front. Optoelectron. 2019, 12(2): 215–226
https://doi.org/10.1007/s12200-019-0824-6

REVIEW ARTICLE

Reflectometric and interferometric fiber optic sensor's principles and applications

Muhammad Noaman ZAHID, Jianliang JIANG (✉), Saad RIZVI

School of Optics and Photonics, Beijing Institute of Technology, Beijing 100081, China

Abstract Fiber optic sensors have been widely used and studied in recent times. This paper presents operating principles and applications of fiber optic sensors namely reflectometric and interferometric fiber optic sensors. Majority of optical fiber sensors fall under these two broad categories. Both interferometric and reflectometric fiber optic sensors are becoming popular for their ease of use, flexibility, long distance sensing, and potentially noise free detection. Also, these sensors can easily be used in various applications such as structural health monitoring, perimeter intrusion detection, temperature monitoring, and other numerous applications. This paper broadly classifies fiber optic sensors into two subtypes. The paper further highlights different sensors based on their sensing resolution, range, spatial advantages, and applications.

Keywords fiber optic, reflectometric, interferometric, optical fiber sensors, sensor applications

1 Introduction

1.1 Fiber optic sensor

The optical fiber sensors have grown enormously as a vital field in engineering. There is a lot of research work present in the form of publications appearing in various conferences and journals. Under such wide expansion in the field it is difficult for scientists and engineers to gain knowledge of where the technology is going relevant to fiber optic sensors. Therefore, this paper highlights key fiber optic sensors and then spotlight fiber optic sensors on the basis of reflectometric and interferometric properties. The paper highlights the key types of such sensors and also focuses on their design technology. Fiber optic sensor are widely used to monitor wide range on environmental phenomenon such as temperature, acoustics, rotation rate, stress, strain, pressure, etc. These sensors have been used to detect gas leakages [1], recognize intrusion patterns [2], and structural health monitoring [3]. Fiber optic sensors comes with an advantage of passive, light weight, compact size, greater temperature performance, high sensitivity, and high bandwidth.

1.2 Sensor classification

Fiber optic sensors have been classified under many different types using different number of approaches in the past. Classification is necessary to categorize different types of fiber optic sensing systems that exist today. A lot of different categories emerged based on the sensor type, working principle, type of optical excitation, detection schemes, and other related factors.

In an early approach, Gaillorenzi et al. [4] discussed the very basic characterization of fiber optic sensors during the time of 1982.

Spooncer et al. classified these sensors based on modulation scheme [5] and argues that different parameters such as polarization, intensity, or rate can be used to classify sensors.

In Ref. [6], Udd characterized these sensors as extrinsic and intrinsic sensors. According to literature, extrinsic sensors are those in which fiber acts as guided medium but the interaction of light with physical quantity is outside the fiber. Whereas, intrinsic fiber optic sensors the sensing mechanism is carried out within the fiber.

Inside the intrinsic fiber optic sensor, there lies the category of interferometric fiber optic sensors. Interferometric sensors have been long used to measure different types of parameters. The intrinsic sensor depends on the use of guiding medium whether it is single mode fiber or a multi-mode fiber. Also the characteristics of light are important in such sensors specially related to interferometric properties of sensor itself, such as coherence of

Received April 28, 2018; accepted November 14, 2018

E-mail: jiangjianliang@bit.edu.cn

light. Light can be highly coherent or of low coherence, affects the operational principle of the sensor. Based on the subdivisions of the sensors in Ref. [6], intrinsic and extrinsic sensors are characterized as shown in Figs. 1 and 2.

Further categorization of fiber optic sensors can also be chalked down to a level of measurement, whether the sensor detects a single point or is a distributed sensor. In a distributed fiber optic sensor, multi-points can be detected for different applications and measuring different parameters. Normally these distributed sensors are used to pick up effects across the length of the fiber. Another subdivision of distributed sensors is the quasi-distributed sensors, in which normal single point sensors are cascaded to form a distributed solution along the length of the fiber. Quasi-distributed sensors are used to measure different phenomenon such as acoustics, acceleration, strain, and temperature [6].

However, the major category which is presented in this paper involves interferometric sensors, which can be classified as shown in Fig. 3.

2 Reflectometric techniques

Fiber optic sensors based on this technique are also categorized as distributed sensors. These sensors use the principle of optical ranging. One of the most key technique

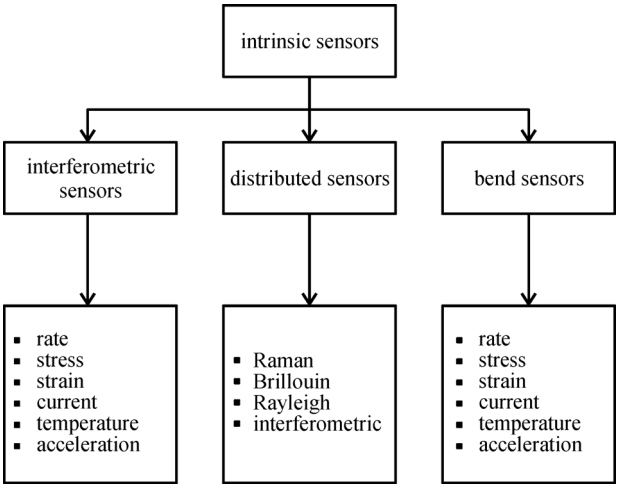

Fig. 1 Block diagram of intrinsic sensors

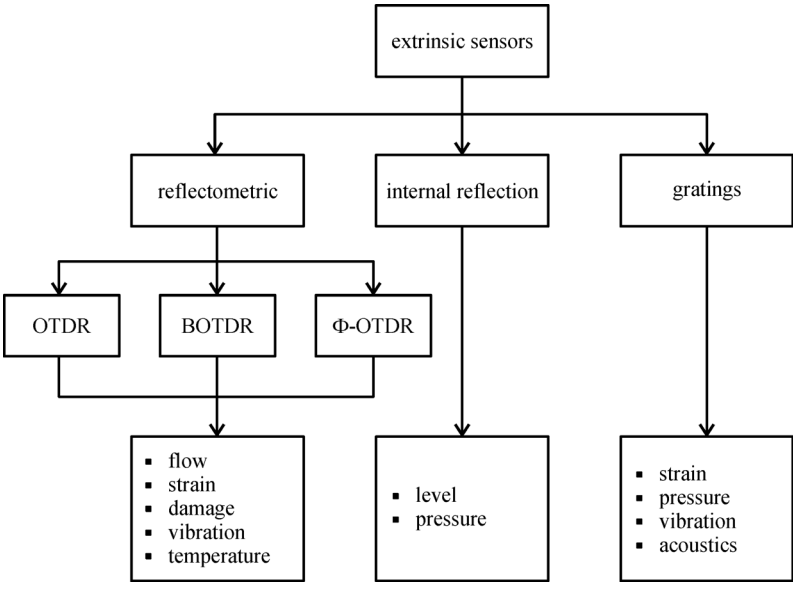

Fig. 2 Block diagram of extrinsic sensors. OTDR: optical time domain reflectometry; BOTDR: Brillouin optical time domain reflectometry; Φ-OTDR: phase-sensitive optical time-domain reflectometry

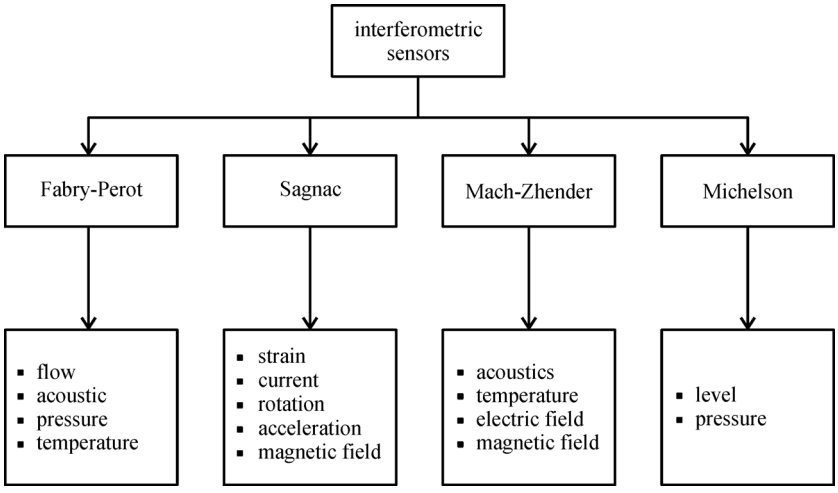

Fig. 3 Block diagram of interferometric sensors

for optical ranging by using reflectometric principle is the optical time domain reflectometry (OTDR).

Among reflectometric techniques, Brillouin and Raman scattering based sensors are well known. These sensors make use of nonlinear interaction of light with fiber material. In principle, if a light of wavelength is imparted into a fiber, a very small amount of light is scattered back from every point in the fiber during its propagation. Alongside the injected wavelength (called Rayleigh component), other wavelength are also generated called the Brillouin and Raman components. The other components generated from original light are shifted in wavelength and contains information about the points of reflection in fiber such as temperature, strain, etc. In Raman scattering based sensors, the scattered component's peak is temperature dependent. Thus local temperature can be figured out by processing intensity peaks of Raman components. Whereas, in Brillouin sensor, Brillouin scattering is the interaction of light and ultrasound waves in the fiber. The wavelength shift on Brillouin component is proportional to the acoustic velocity in the fiber that is linked to strain and temperature of the fiber. Thus, Brillouin shift is used to measure temperature and strain.

2.1 Optical time domain reflectometry (OTDR)

Light is guided in the optical fiber usually using coherent narrow band source. Due to microscopic variation in fiber geometry, the light suffers loss called Rayleigh scattering in the fiber. The scattered light is partially reflected back in the direction of light propagation, and is captured by the fiber. This light traveling back toward the source can be further processed. The optical source is operated in pulsating mode and variation in the scattered light returning back through scattering and reflection is monitored. The signal captured at the detector can be processed further through signal processing techniques and this is the basic principle of optical time domain reflectometry (OTDR). OTDR technique was used mainly for fault tracing in optical cables [7,8]. Figure 4 shows the OTDR system configuration.

A short pulse is sent into the fiber using laser diode. The digital signal processing (DSP) electronics monitors the backscattered signal with respect to time compared to input pulse. In case of no non-uniformity, the backscattered signal decays with time due to losses in the fiber. In case of fault or breakage in the fiber, multiple point reflections

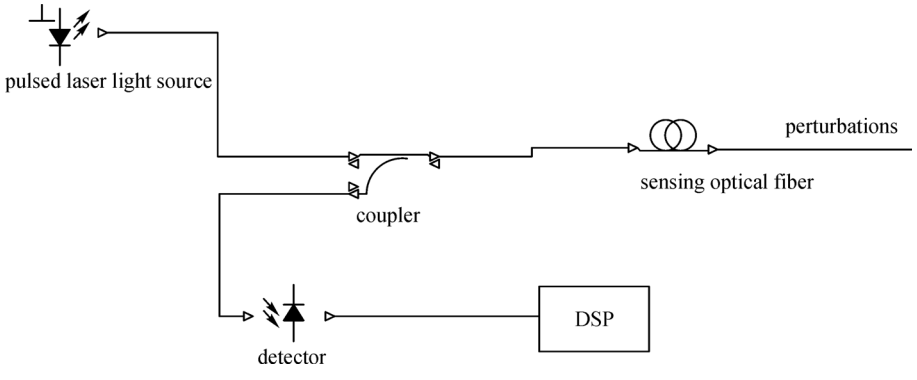

Fig. 4 Configuration of OTDR system

occur, that can be detected at the detector, and the signal curve can be processed with respect of time to compute distance of fault. Signals produced by OTDR are weak and require averaging of many samples to give substantial accurate results.

The backscattered signal for such reflectometric system is given by

$$P_s(t) = (1-k)k(P_0 Dr(z))\exp\left\{-\int_0^z 2\alpha(z)\mathrm{d}z\right\}, \quad (1)$$

where z is the location of the forward propagating light beam, $P_s(t)$ is the backscattered signal, α is the attenuation coefficient.

A simple OTDR is used to measure any perturbation along the fiber length. Whereas, the Brillouin optical time domain reflectometry (BOTDR) is widely used for strain and temperature measurement.

2.2 Brillouin optical time domain reflectometry (BOTDR)

The Brillouin optical time domain reflectometry (BOTDR) shown in Fig. 5, sometimes referred to as optical fiber strain analyzer, is a well-known single ended access to the source and detection systems that provide Brillouin gain loss based on distribution sensors, such as the use of Rayleigh scattering effect in standard OTDR sensors. Currently the optical fiber sensing technology based on BOTRD has been widely used as distributed monitoring methods. Recently, BOTDR instruments are suitable for measuring the strain over a certain distance.

BOTDR is also used to monitor strain in health monitoring applications. An example of such technique is given by Ref. [9] where deformation of tunnel is measured using reflectometric properties of light along a distributed optical fiber. Fiber is laid to detect cracks and damage along multiple points with a resolution of 1 m. BOTDR proved to be good for fault tracing or damage detection. However, one drawback of this technology is that its long time monitoring. A room for improvement exists in using BOTDR for its application.

Another study [10] demonstrates the use of reflectometric fiber optic technology using BOTDR to measure distributed strain along the optical fiber deployed over pipeline. The sensor has been used to detect crack in a concrete structure by detecting strain through optical fiber with high resolution.

BOTDR is a useful technique which evaluates temperature measurement and strain events in optical cables up-to 80 km. Different types of fibers have their own characteristic Brillouin spectrum. Techniques are described to allow the use of BOTDR for different corning fiber types including those with spectra that contain more than one maxima [11].

2.3 Phase-sensitive optical time domain reflectometry (Φ-OTDR)

The phase-sensitive optical time-domain reflectometry (Φ-OTDR) shown in Fig. 6, is a primary example of standard distributed optical fiber sensing systems [12]. Such distributed fiber optic sensors (DOFS) are used for many applications such as fault detection in optical fibers, perimeter intrusion detection, pipeline safety monitoring [13], etc. For vibration sensing, Φ-OTDR can detect distributed perturbations along the fiber [14]. These distributed sensors are superior to traditional point based schemes and holds a great potential for large scale monitoring, low price per monitored point, easy installation, and geometric versatility [15,16]. In Φ-OTDR, a highly coherent pulse light is injected into the sensing fiber which then reflects down the fiber to produce optical power curve for monitoring [17]. The measurement of interference variation provides Φ-OTDR with a high sensitivity compared with other DOFS systems. Therefore, Φ-OTDR is deployed underground for applications such as vibration detection and monitoring parameters of moving [18,19]. Besides, Φ-OTDR is able to acquire an ultra-long sensing range. The longest repeater-less DOFS has been demonstrated in the form of Φ-OTDR [20].

An interesting application of reflectometric sensors is in the area of distributed acoustic sensing. These systems send continuous pulses of light into fiber and capture the rerun signal which has scattered within the fiber. This backscattered signal can be processed in terms of phase,

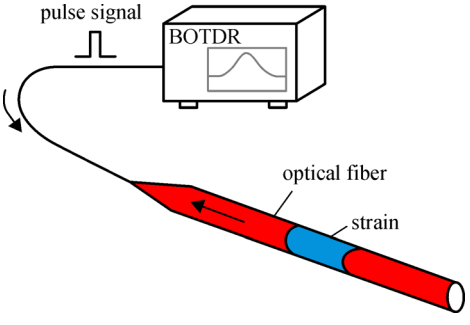

Fig. 5 Configuration of BOTDR

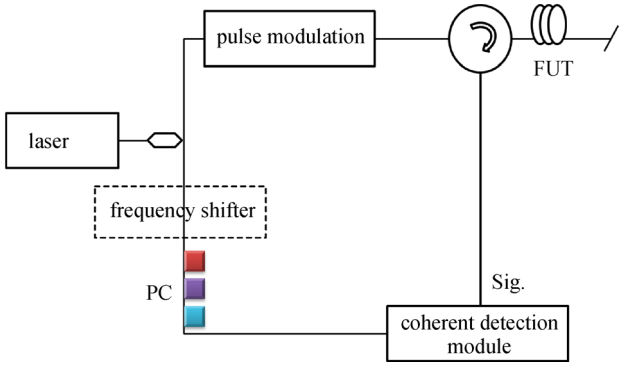

Fig. 6 Configuration of Φ-OTDR

forming phase sensitive optical time domain reflectometer (Φ-OTDR). The sensor inputs a laser of narrow line-width, and processes the change in phase of the returning Rayleigh signal [21 – 23].

Brillouin based BOTDRs are also used to determine acoustic signals [24]. However these sensors cannot completely capture the acoustic field. For complete acoustic imaging, phase, frequency, and amplitude information are required. To completely determine acoustic signatures, interferometric techniques proof to be more reliable and powerful [25].

2.4 Application

Most of the reflectometric sensors are classified under the category of distributed fiber optic sensor. These sensors have been used to monitor the health condition of dams, bridges, and other civilian structures. These dams, bridges, and other structures get deteriorated with time and needs maintenance at right time, before a major damage is done. Conventional methods can detect such changes at larger scale and cannot pinpoint the point of damage to these structures. Therefore, fiber optic reflectometric sensors have replaced conventional sensors as these sensors are used for temperature, strain, vibration, and leakage sensing.

3 Interferometric techniques

Interference is the main phenomenon in these sensors. The interferometric sensors work by measuring interference between beams of light. In an interferometer, the light input is split up into two paths and travels along them. The two beams traveling are then recombined at the output. The total electric field vector is given by

$$E = E_1 + E_2, \tag{2}$$

where

$$E_1 = E_1 \mathrm{e}^{\mathrm{j}(wt+Ø1)}, \tag{3}$$

$$E_2 = E_2 \mathrm{e}^{\mathrm{j}(wt+Ø2)}. \tag{4}$$

The intensity of the interference is given by

$$I = c\varepsilon_0 \langle E \cdot E^* \rangle, \tag{5}$$

$$I = I_1 + I_2 + \sqrt{I_1 I_2}\cos\Delta Ø. \tag{6}$$

When the two beams are in phase, the intensity at the output is maximum:

$$I_{\max} = I_1 + I_2 + 2\sqrt{I_1 I_2}. \tag{7}$$

Whereas, when the two beams are opposite in terms of phase, the output is given by

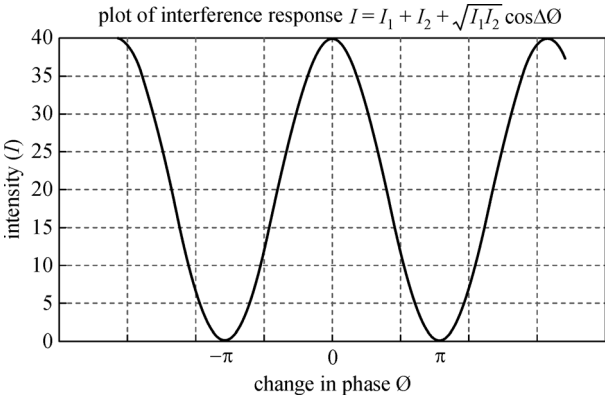

Fig. 7 Interferometer response

$$I_{\min} = I_1 + I_2 - 2\sqrt{I_1 I_2}. \tag{8}$$

The response of interferometer in terms of phase difference between the two waves is shown in Fig. 7 This sinusoidal response can be seen at the interferometric detector end. Moving this response in the linear region via modulation is often utilized in designing sagnac interferometers as discussed further.

Interferometry technique is very sensitive method for measuring different parameters. There are four broad categories of interferometric sensor which are based on: Michelson interferometer, Fabry-Perot interferometer, Sagnac interferometer, and Mach-Zhender interferometer.

3.1 Sagnac interferometer

Sagnac interferometers are used to sense a wide range of environmental phenomenon. Fiber based gyros on this approach are widely used for inertial measurements for navigation purposes. The Sagnac interferometer provides rotation sensing in these applications. However, sensors based on Sagnac effect are also used for measuring acoustic [26], magnetic [27], strain, and acceleration [28]. However, optical rotation sensing is the main application of Sagnac interferometry [29,30].

In Sagnac interferometer (Fig. 8), two counter-propagating beams within a ring of radius R interfere to give rotation information. If the ring rotates at a rate given by Ω in clock-wise direction, then the clockwise beam travels a path of length $2\pi R + \Omega R\Delta t$ and counter-clockwise beam travel $2\pi R - \Omega R\Delta t$. Thus path difference between two beams is given by $2\Omega RL/c$. To measure rotation effect, the optical sensor should be designed carefully and environmental conditions require to be set for rotation measurement only. Rotation sensors are being configured using three main configurations:

1) Open-loop interferometers;
2) Optical resonators;
3) Closed-loop interferometer scheme.

In open loop scheme, the path length is divided by

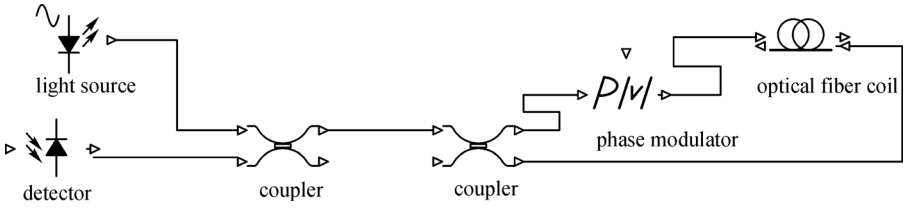

Fig. 8 Sagnac interferometer configuration

operating wavelength to give the number of fringes of phase difference between counter-propagating waves induced by rotation. The open loop scheme is used for achieving lower dynamic range and scale factor accuracy. This scheme is used for low level applications such as platform stabilization, control of robot, and tracking [31,32].

The resonator type sensor is formed on the basis of meeting resonant condition, having integral number of waves around on optical circuit with clock-wise and counter-clockwise beams forming relationship with wavelength and rate as

$$F = F_{\mathrm{cw}} - F_{\mathrm{ccw}} = 2R\Omega/\lambda, \tag{9}$$

where F_{cw} is the frequency number for clockwise beam and F_{ccw} is the frequency number for counter-clockwise beam.

The equation above is valid for the passive ring resonator and ring laser gyroscopes. Ring laser gyros [33,34] are also important in navigational applications and are very precise. The lasing condition inside the optical ring cavity has integral number of waves inside one complete optical circuit. The frequency, wavelength, and area change in the sensor is given by

$$-\frac{\mathrm{d}v}{v} = \frac{\mathrm{d}\lambda}{\lambda} = \frac{\mathrm{d}P}{p}. \tag{10}$$

The equation above computes the change in perimeter in a ring laser and is the fundamental equation on which sensor is based. The increase and decrease in path length is given by

$$\mathrm{d}P = 2A\Omega/(nc), \tag{11}$$

where A is the area of close path, c is the rotation rate and n is index of refraction.

In contrast to ring based gyros that measure Sagnac effect by measuring change in circuit path-length of a single circuit, the fiber optic gyro [35] measures Sagnac effect in a scheme with fiber coil having many turns. The fiber optic gyros are passive devices without a resonant cavity with external optical source from the sensing medium. Broadband light source is used in such configurations, unlike ring resonators which require a lasing condition for operation. In close-loop operation fiber optic interferometric rotations sensor [36] operates by using a phase nulling scheme. The rotationally produced phase difference is nulled by an opposite balancing phase shift. The close-loop scheme increases the dynamic range of open-loop sensors by processing even and odd harmonic and processing non linearity.

3.2 Mach-Zhender interferometers

Most of the fiber interferometric sensors employ Mach-Zhender scheme. However, Mach-Zhender scheme comes with complexity and other schemes offer advantages over Mach-Zhender scheme. Mach-Zhender is the easiest realization of the interferometric principle.

In Mach-Zhender interferometer, a coherent single-mode laser optical source is injected into the fiber. The light is split onto two beams of nominal equal intensity by a coupler (or beam splitter). The light is split into equal intensity, with one beam sent into the sensing arm and other into the reference arm. These beams after passing through the two arms are then combined through a coupler and there is an interference pattern generated at the detector. To achieve high performance, such sensor has long length of fiber. The change in length disturbs the output at detectors and, hence, generates a phase difference, which can be further processed. The optical phase delay is related to length of fiber in which light travels through:

$$Ø = nkL, \tag{12}$$

where nL is the optical path length and Ø is the optical phase delay. Figure 9 shows basic configuration. The sensing arm is used to generate phase shift of interest, whereas, the reference arm provides reference path.

Mach-Zhender interferometer scheme is used in different configurations [37,38]. In Ref. [37], the Mach-Zhender configuration is used to measure magnetic field and acoustic sensing. In this configuration, the sensing fiber is similar to the reference fiber. The response of both the arms is similar. In the absence of any perturbation, the uniform field would generate no output at the sensor. In case, when there is varying field across the separation of the two fiber coils, a gradient change is present at the output. The gradient change is computed by processing the phase shift of the interferometer. The sensor is a prime example of optical sensor power as it subtracts the signal from each coil optically. The best performance of the sensor is achieved when the reference arm is matched with

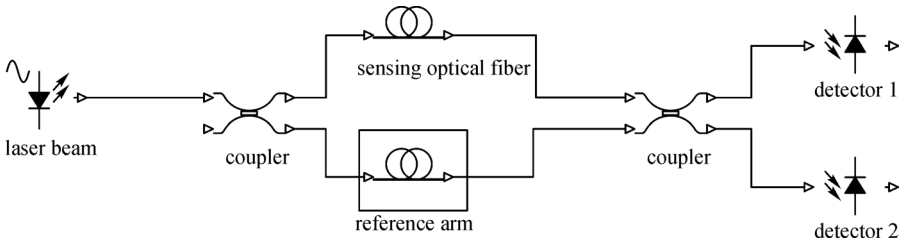

Fig. 9 Mach-Zhender interferometers configuration

the sensing arm of the sensor. Recently, an advanced sensor using Mach-zhender interferometers for magnetic field measurements has also been demonstrated [39].

Another type of sensor utilizing Mach-Zhender scheme is the push-pull type design [38]. In this sensor, an enhanced optical phase shift is generated through the scheme of setting normalized setting parameters. If the normalized sensitivity parameter of the sensing arm is R, and that of reference arm is $-R$, then a resultant optical phase shift is doubled. However, the scheme demands sophistication of design as it is difficult to get $-R$ response.

3.3 Michelson interferometer

Michelson interferometer is a common configuration of optical interferometry, Albert Abraham Michelson invented this configuration topology. Physical distance can be measured by using this type of configuration, directly in terms of wavelength (λ) of laser beam by calculating interference fringes. It is necessary that beam must be mutually coherent and have a phase relationship. In Michelson interferometer, beam splitter is used for splitting the light into two different optical paths originated from laser beam, in this way we can obtain mutual coherence. Transmitted and reflected waves are recombined; they interfere and form interference in focal plane.

A typical configuration of Michelson interferometer is shown in Fig. 10. A beam splitter that is partially reflected mirror is placed at the angle of 45° to the incoming laser beam. Half (50%) of the light is transmitted through to mirror (M1) while the remaining half (50%) of light is reflected in the direction of mirror (M2). Both beams recombine and directed toward screen to produce interference fringes on the screen.

At the center of the screen max intensity can be calculated as

$$2D = n\lambda, \tag{13}$$

also,

$$\lambda = 2D/n, \tag{14}$$

where λ is wavelength, D is distance of moveable objects (M1 and M2) in mm and n is the number of fringes.

An advantage of Michelson interferometer compared to other schemes (like Mach-Zhender) is the ease of

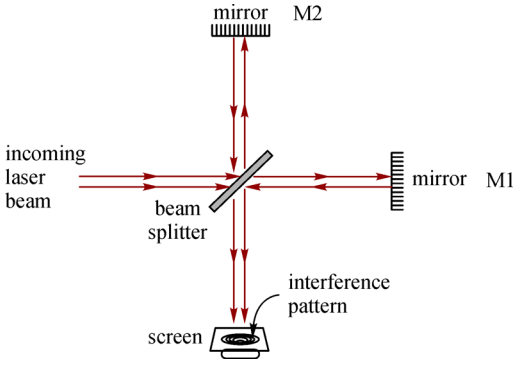

Fig. 10 Michelson interferometer configuration

construction, as it requires only one coupler as shown in Fig. 11. This figure presents a fiber based model of Michelson interferometer. As the light passes through the sensing and reference arms twice, the optical phase shift is doubled. At the end of both the arms of the sensor, there is a mirror that reflects back the light. Light traverses through sensing arm and reference arm and is reflected back. These reflected signals from both the arms are combined at the coupler. The output in term of phase change can be processed for sensing at the port with which detector is connected. Therefore, normal Michelson sensor has intrinsic optical phase shift R_{tot} equal to R, and with push-pull configuration it can become $2R$. Michelson interferometer based sensor is easy to package. The sensor can also be activated with single fiber between the sensor and source/detector. In terms of disadvantage, Michelson interferometer needs mirrors that are not easily available commercially and needs to be fabricated. Also, the light reflected back is also fed as a high input to the source, which is not a practical design.

For detection of gravitational wave, the Michelson interferometer is leading method. For validation of gravitational waves an interferometer is used [40] to detect cosmic gravitational waves.

Michelson interferometer is also used in optical coherence tomography (OCT), based on low-coherence interferometry [41], tomographic visualization of internal tissue microstructures can be provided in medical imaging technique.

In Fig. 12, OCT instrument is constructed by using Michelson interferometeric configuration. Low coherence

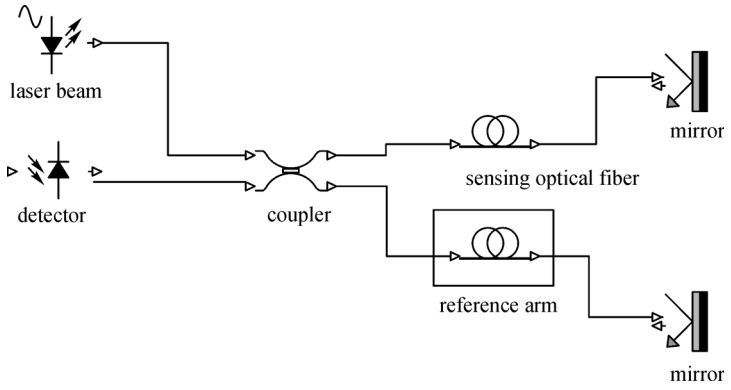

Fig. 11 Michelson interferometer configuration

light source is used and interference is detected with the help of photodiode (detector). Light originated from the source in OCT system is divided into two arms. A sample arm emits a beam that is directed toward the item of interest (which is being imaged) and scanned while the other arm is reference arm with scanning optical delay line.

For research applications in OCT system, for OCT imaging short pulse lasers are preferred as light sources because they have following advantages; high speed imaging, high output power, high resolution and extremely short coherence lengths [42]. For clinical application semiconductor based light sources are preferred than the short pulse lasers. With advancements in micro optical electro mechanical system MOEMS technology, miniaturized Michelson interferometers for OCT applications have also been demonstrated [43].

With the help of Michelson interferometer which consist of fiber optic power divider, velocity and vibration can be measured [44]. For vibration measurement, the sensor is used for measuring very low order displacements with very high accuracy. The information about the vibratory objects is transmitted through optical probe in this interferometer in the form of Doppler beat signal [45]. In this interferometer configuration, two fibers are twisted together and put under the tension.; To evaluate the fiber-optic power divider, He-Ne laser is used for linearly polarized light at the input port of power divider. At the input and output ends, index matching gel is mounted as cladding mode stripper.

Figure 13 shows the schematic diagram of fiber optic Michelson interferometer which consist an optical power divider that is used for measuring the vibration of moveable mirror. Port 1 of the power divider is used as input port at which He-Ne laser light launched and then coupling section passes this light toward port 3 and port 4. There is a voice coil at output of port 4 on which vibratory mirror is mounted. A lens is used at the output of port 4 to focus the light for the vibratory mirror. At port 3 fixed mirror is used, some portion of light from this port and light from port 4 combined and propagate down toward port 2. Where photo multiplier is used to detect the superimposed phase front of interference pattern. When the vibration of object is sinusoidally in the beam axis's direction, the instantaneous Doppler beat frequency is

$$\Delta f = (2\xi\omega/\lambda)\cos\omega t, \tag{15}$$

where ζ is peak amplitude of vibratory object, ω is angular frequency and λ is wavelength in free space.

During every half cycle of displacement, there is 2π change in phase of Doppler beat signal. By using above mentioned equation, the max deviation of the beat frequency is

$$\Delta f_{\max} = 2\xi\omega/\lambda. \tag{16}$$

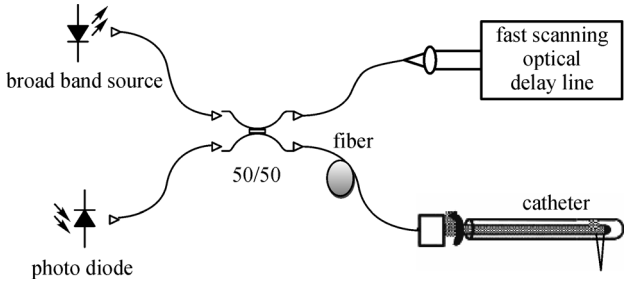

Fig. 12 OCT instrument using Michelson interferometer configuration

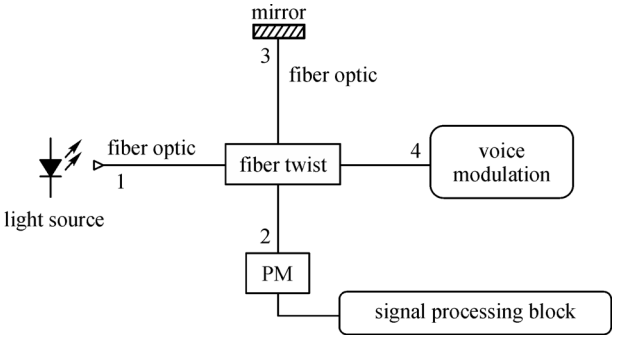

Fig. 13 Michelson interferometer configuration using optical power divider. PM: phase modulator

Another application of such sensor can be for temperature sensing. A Michelson based fiber optic thermometer was demonstrated in Ref. [46] and temperature probe in Ref. [47].

3.4 Fabry-Perot interferometer

Fabry-Perot based sensors [48] are not commonly used due to design drawbacks. It is also an example of multi-beam interferometric sensor like the ring resonator design. The configuration of Fabry-Perot design is shown in Fig. 14. In Fabry-Perot sensor, as shown in the figure, the mirrors are highly reflective, making light resonates back and forth in the cavity between the mirrors, causing phase delay in the cavity multiple times. The output that is transmitted with phase shift in terms of intensity is dependent on the transmission (T) and reflection (R) coefficient of the mirrors. The intensity is given by

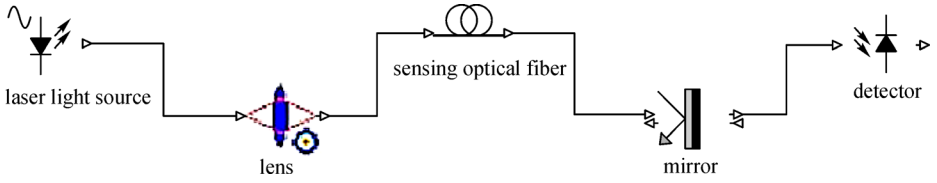

Fig. 14 Fabry-Perot configuration

Table 1 Summary of reflectometric and interferometric fiber optic sensors

	types	applications
relectometric techniques	OTDR	for return loss measurements [57]
	BOTDR	for testing fiber optic cables
		widely used for optical cable maintenance and construction
		can be used for sensing chemicals and gases
		the strain that arises when laying submarine optical fiber cable can be measured [58]
	Φ-OTDR	detection of earthquake damage [59]
		the strain in frozen telecommunications cable can determined [59]
		for structural monitoring [60]
		optical fiber sensor system for river levee collapse detection [61]
		well suited for underground deployments [62]
		for use of intrusion detection or high-speed train monitoring [63]
		abnormal vibration detection along oil/gas pipes [64–67]
		intrusion alarm and location system [64–67]
		distributed acoustic test for train tracking [64–67]
interferometric techniques	Fabry-Perot	thermospheric/ionospheric measurements [68]
		vibration measurements [45,46]
	Sagnac	optical rotation sensing [29,30]
		acoustic measurements [26]
		magnetic measurements [27]
		strain and acceleration measurements [28]
	Mach-Zhender	used to measure magnetic field and acoustic sensing [37]
		used in optical processing of signals like switching, add drop multiplexing, modulators [69]
		to monitor the extent of deformation in the nanometer scales during the reaction [70]
	Michelson	for detection of gravitational waves [40]
		in astronomical interferometry [40]
		in optical coherence tomography [41]
		velocity and vibration can be measured [44]
		as the core of Fourier transform spectroscopy [71]

$$I(\text{Ø}) = \frac{A^2T^2}{(1-R^2)1 + \left[\frac{4R}{(1-R)^2}\right]\sin^2\text{Ø}.} \quad (17)$$

The Fabry-Perot senor has better sensitivity compared to the Mach-Zhender due to its cavity finesse giving better phase detection capability. Fabry-Perot sensors with cavity finesse have been demonstrated [49] to achieve high sensitivity.

However, Fabry-Perot based sensors are not very practical. These sensors have are not practical due to sensitivity to the coherence length of the source and frequency jitters, complex intensity function $I(\text{Ø})$. The Fabry-Perot sensor cannot be used with diode laser sources, as the sensitivity of the sensor is very low. Thus, the sensor is not used in high sensitivity applications. The detection schemes for Fabry-Perot sensor also requires complex stages, as no passive technique has be developed for such complex intensity transfer function give above.

However, with advancements in technology and advent of specialty fibers, the Fabry-Perot scheme became more and more practical and recently some sensors have been demonstrated for application like vibration measurement [50,51].

3.5 Applications

The interferometric sensors have been used in a variety of applications. These sensors can detect many alternating current parameters such as vibrations/acoustics [52], magnetic fields [53], electric sensing [54], flow of current [55], and strain [56]. In terms of current parameters, the interferometric sensors have been shown to sense Coriolis flow [57].

The two-beam sensors such as Michelson and Mach-Zhender are used for high sensitivity applications. They are used in many applications for sensing high sensitive temperature, pressure, acoustics, acceleration etc.

4 Conclusions

In this paper, we discussed the reflectometric and interferometric fiber optic sensors and classified them under sub types such as optical time domain reflectometry (OTDR), Brillouin optical time domain reflectometry (BOTDR), Sagnac interferometer, Mach-Zhender interferometer, Michelson interferometer and Fabry-Perot interferometer. We presented an overview of some important applications of these sensors in the field of medical, physics and electronics. Most popular trends have been seen in rotation sensing (for interferometry), fault tracing and perimeter intrusion detection (for OTDR type sensors) and, imaging technology (for Michelson type sensors). Beside discussion of various applications, we have also summarized their working principles, practical implementations and techniques of these key sensors.

Acknowledgements We would highly acknowledge the contribution of Saad Rizvi in directing this paper based on his technical knowledge of the field.

References

1. Bévenot X, Trouillet A, Veillas C, Gagnaire H, Clément M. Hydrogen leak detection using an optical fibre sensor for aerospace applications. Sensors and Actuators. B, Chemical, 2000, 67(1–2): 57–67
2. Kwon I B, Baik S J, Im K, Yu J W. Development of fiber optic BOTDA sensor for intrusion detection. Sensors and Actuators A, Physical, 2002, 101(1-2): 77–84
3. Guo H, Xiao G, Mrad N, Yao J. Fiber optic sensors for structural health monitoring of air platforms. Sensors (Basel), 2011, 11(4): 3687–3705
4. Gaillorenzi T G. Optical fiber sensor technology. IEEE Journal of Quantum Electronics, 1982, 8: 626–660
5. Spooncer R C. Fiber optics in instrumentation. In: Sydenham P H, Thorn R, eds. Handbook of Measurement Science. Chichester: Wiley, 1992
6. Udd E. Fiber Optic Sensors. New York: Wiley, 1991
7. Marcuse D. Principle of Optical Fiber Measurements. New York: Academic Press, 1981, Chap. 5
8. Barnoski M K, Jensen S M. Fiber waveguides: a novel technique for investigating attenuation characteristics. Applied Optics, 1976, 15 (9): 2112–2115
9. Shi B, Sui H, Liu J, Zhang D. The BOTDR based distribution monitoring system for slope engineering. In: Culshaw M G, Reeves H J, Jefferson I, Spink T W, eds. Engineering Geology for Tomorrow's cities. London: Geological Society, 2009
10. Yasue N, Naruse H, Masuda J, Kino H, Nakamura T,Yamaura R. Concrete pipeline strain measurement using optical fiber sensor. IEICE Transactions on Electronics, 2000, 83(3): 468–474.
11. Kurashima T, Horiguchi T, Izumita H, Furukawa S I, Koyamada Y, Brillouin optical-fiber time domain reflectometry. IEICE Transactions on Communications, 1993. E76-B(4), 382–390
12. Park J, Lee W, Taylor H F. A fiber optic intrusion sensor with the configuration of an optical time domain reflectometer using coherent interference of Rayleigh backscattering. Proceedings of the Society for Photo-Instrumentation Engineers, 1998, 3555: 49–56
13. Wu H J, Wang Z N, Peng F, Peng Z P, Li X Y, Wu Y, Rao Y J. Field test of a fully distributed fiber-optic intrusion detection system for long-distance security monitoring of national borderline. In: Proceedings of 23rd International Conference on Optical Fibre Sensors, Santander, Spain, 2014
14. Juarez J C, Maier E W, Choi K N, Taylor H F. Distributed fiber-optic intrusion sensor system. Journal of Lightwave Technology, 2005, 23 (6): 2081–2087
15. Thévenaz L. Review and progress on distributed fiber sensing. In: Optical Fiber Sensors. OSA Technical Digest (Optical Society of America), Cancun Mexico, 2006, ThC1

16. Zhu T, He Q, Xiao X, Bao X. Modulated pulses based distributed vibration sensing with high frequency response and spatial resolution. Optics Express, 2013, 21(3): 2953–2963
17. Martins H F, Martin-Lopez S, Corredera P, Salgado P, Frazão O, González-Herráez M. Modulation instability-induced fading in phase-sensitive optical time-domain reflectometry. Optics Letters, 2013, 38(6): 872–874
18. Wu H, Wang Z, Peng F, Peng Z, Li X, Wu Y, Rao Y. Field test of a fully-distributed fiber-optic intrusion detection system for long-distance security monitoring of national borderline. Proceedings of the Society for Photo-Instrumentation Engineers, 2014, 9157: 915790–915791
19. Duan N, Peng F, Rao Y, Du J, Lin Y. Field test for real-time position and speed monitoring of trains using phase-sensitive optical time domain reflectometry (Φ-OTDR). Proceedings of the Society for Photo-Instrumentation Engineers, 2014, 9157: 1–4
20. Wang Z N, Zeng J J, Li J, Fan M Q, Wu H, Peng F, Zhang L, Zhou Y, Rao Y J. Ultra-long phase-sensitive OTDR with hybrid distributed amplification. Optics Letters, 2014, 39(20): 5866–5869
21. Juarez J C, Maier E W, ChoiK N, Taylor H F. Distributed fiber-optic intrusion sensor system. Journal of Lightwave Technology, 2005, 23 (6): 2081–2087
22. Juarez J C, Taylor H F. Field test of a distributed fiber-optic intrusion sensor system for long perimeters. Applied Optics, 2007, 46(11): 1968–1971
23. Peng F, Cao X. A hybrid phi/B-OTDR for simultaneous vibration and strain measurement. Photonics Sensors, 2016, 6(2): 121–126
24. Bao X, Chen L. Recent progress in optical fiber sensors based on Brillouin scattering at University of Ottawa. Photonic Sensors, 2011, 1(2): 102–117
25. Liu X, Wang C, Shang Y, Wang H. Distributed acoustic sensing with Michelson interferometer demodulation. Photonics Sensors, 2017, 7(3): 193–198
26. Ma J, Yu Y, Jin W. Demodulation of diaphragm based acoustic sensor using Sagnac interferometer with stable phase bias. Optics Express, 2015, 23(22): 29268–29278
27. Lv F, Han C, Ding H, Wu Z, Li X. Magnetic field sensor based on microfiber Sagnac loop interferometer and ferrofluid. IEEE Photonics Technology Letters, 2015, 27(22): 2327–2330
28. Wada K, Narui H, Yamamoto D, Matsuyama T, Horinaka H. Balanced polarization maintaining fiber Sagnac interferometer vibration sensor. Optics Express, 2011, 19(22): 21467–21474
29. Post E J. Sagnac effect. Reviews of Modern Physics, 1967, 39(2): 475–493
30. Arditty H J, Leèfovre H C. Sagnac effect in fiber gyroscopes. Optics Letters, 1981, 6(8): 401–403
31. Kersey A D, Dandridge A, Burns W K. Two-wavelength fibre gyroscope with wide dynamic range. Electronics Letters, 1986, 22 (18): 935–937
32. Kim B Y, Lefevre H C. Harmonic feedback approach to fiber optic gyro scale factor stabilization. In: Proceedings of IEEE Conference on Optical Fiber Sensors, 1983, 136
33. Aronowitz F. The Laser Gyro. In: Ross M, ed. Laser Applications. New York: Academic Press,113–200
34. Chow W W, Gea-Banacloche J, Pedrotti L M, Sanders V E, Schleich W, Scully M O. The ring laser gyro. Reviews of Modern Physics, 1985, 57(1): 61–104
35. Ezekiel S, Arditty H J, eds. Fiber-Optic Rotation Sensors, Springer Series in Optical Sciences, vol. 32. New York: Springer-Verlag, 1982
36. Cahill R F, Udd E. Phase-nulling fiber-optic laser gyro. Optics Letters, 1979, 4(3): 93–95
37. Koo K P, Sigel G H. A fiber optic magnetic gradiometer. Journal of Lightwave Technology, 1983, 1(3): 509–513
38. Tveten A B, Dandridge A, Davis C M, Giallorenzi T G. Fiber optic accelerometer. Electronics Letters, 1980, 16(22): 854
39. Ding X Z, Yang H Z, Qiao X G, Zhang P, Tian O, Rong Q Z, Nazal N A M, Lim K S, Ahmad H. Mach-Zehnder interferometric magnetic field sensor based on a photonic crystal fiber and magnetic fluid. Applied Optics, 2018, 57(9): 2050–2056
40. Miller M C. Gravitational waves: dawn of a new astronomy. Nature, 2016, 531(7592): 40–42
41. Riederer S J. Current technical development of magnetic resonance imaging. IEEE Engineering in Medicine and Biology Magazine, 2000, 19(5): 34–41
42. Fujimoto J G, Pitris C, Boppart S A, Brezinski M E. Optical coherence tomography: an emerging technology for biomedical imaging and optical biopsy. Neoplasia, 2000, 2(1): 9–25
43. Maciel M J, Costa C G, Silva M F, Peixoto A C, Wolffenbuttel R F, Correia J H. A wafer-level miniaturized Michelson interferometer on glass substrate for optical coherence tomography applications. Sensors and Actuators A, Physical, 2016, 242: 210–216
44. Imai M, Ohashi T, Ohashi Y. Fiber-optic michelson interference using an optical power divider. Optics letters, 1980, 5(10): 418–420
45. Bucaro J A, Dardy H D, Carome E F. Fiber-optic hydrophone. Journal of the Acoustical Society of America, 1977, 62(5): 1302–1304
46. Corke M, Kersey A D, Jackson D A, Jones J D C. All fibre Michelson thermometer. Electronics Letters, 1983, 19(13): 471
47. Zhao N, Fu H, Shao M, Yan X, Li H, Liu Q, Gao H, Liu Y, Qiao X. High temperature probe sensor with high sensitivity based on Michelson interferometer. Optics Communications, 2015, 343: 131–134
48. Petuchowski S, Giallorenzi T, Sheem S. A sensitive fiber-optic fabry-perot interferometer. IEEE Journal of Quantum Electronics, 1981, 17(11): 2168–2170
49. Stone J. Optical-fibre fabry-perot interferometer with finesse of 300. Electronics Letters, 1985, 21(11): 504–505
50. Xia W, Li C, Hao H, Wang Y, Ni X, Guo D, Wang M. High-accuracy vibration sensor based on a Fabry-Perot interferometer with active phase-tracking technology. Applied Optics, 2018, 57(4): 659–665
51. Zhang Q, Zhu T, Hou Y, Chiang K. All-fiber vibration sensor based on a Fabry Perot interferometer and a microstructure beam. Journal of the Optical Society of America B, Optical Physics, 2013, 30(5): 1211–1215
52. Bucaro J A, Dardy H D, Carome E. Fiber optic hydrophone. Journal of the Acoustical Society of America, 1977, 62(5): 1302–1304
53. Dandridge A, Tveten A B, Sigel G H, West E J, Giallorenzi T G. Optical fiber magnetic field sensor. Electronics Letters, 1980, 16 (11): 408
54. Koo K P, Sigel G H. An electric field sensor utilizing a piezoelectric

PVF2 film in a single-mode fiber interferometer. IEEE Journal of Quantum Electronics, 1982, 18(4): 670–675
55. Dandridge A, Tveten A B, Giallorenzi T G. Interferometric current sensor using optical fibres. Electronics Letters, 1981, 17(15): 523–525
56. Bucaro J A, Lagakos N, Cole J H,Giallorenzi T G. Fiber optic acoustic transduction. Physical Acoustics, 1982, 16(C): 385–457
57. Wade C A, Dandrige A. Fibre-optic coriolis mass flowmeter for liquids. Electronics Letters, 1988, 24(13): 783–785
58. Kurashima T, Horiguchi T, Yoshizawa N, Tada H, Tateda M. Measurement of distributed strain due to laying and recovery of submarine optical fiber cable. Applied Optics, 1991, 30(3): 334–337
59. Kurashima T, Hogari K, Matsuhashi S, Horiguchi T, Koyamada Y, Wakui Y, Hirano H. Measurement of distributed strain in frozen cables and its potential for use in predicting cable failure. In: Proceedings of International Wire & Cable Symposium Proceedings, 1994, 593602
60. Thevenaz L. Monitoring of large structure using distributed Brillouin fiber sensing. In: Proceedings of 13th International Conference on Optical Fiber Sensors, Korea, 1999, 345–348
61. Ohno H, Naruse H, Kihara M, Shimada A. Industrial applications of the BOTDR optical fiber strain sensor. Optical Fiber Technology, 2001, 7(1): 45–64
62. Wu H, Wang Z, Peng F, Peng Z, Li X, Wu Y, Rao Y. Field test of a fully-distributed fiber-optic intrusion detection system for long-distance security monitoring of national borderline. Proceedings of the Society for Photo-Instrumentation Engineers, 2014, 9157: 915790–915791
63. Duan N, Peng F, Rao Y, Du J, Lin Y. Field test for real-time position and speed monitoring of trains using phase-sensitive optical time domain reflectometry (Φ-OTDR). Proceedings of the Society for Photo-Instrumentation Engineers, 2014, 9157: 1–4
64. Peng F, Wu H, Jia X H, Rao Y J, Wang Z N, Peng Z P. Ultra-long high-sensitivity Φ-OTDR for high spatial resolution intrusion detection of pipelines. Optics Express, 2014, 22(11): 13804–13810
65. Tejedor J, Martins H F, Piote D, Macias-Guarasa J, Pastor-Graells J, Martin-Lopez S, Guillén P C, De Smet F, Postvoll W, González-Herráez M. Toward prevention of pipeline integrity threats using a smart fiber-optic surveillance system. Journal of Lightwave Technology, 2016, 34(19): 4445–4453
66. Sun Q, Feng H, Yan X, Zeng Z. Recognition of a phase-sensitivity OTDR sensing system based on morphologic feature extraction. Sensors (Basel), 2015, 15(7): 15179–15197
67. Peng F, Duan N, Rao Y, Li J. Real-time position and speed monitoring of trains using phase-sensitive OTDR. IEEE Photonics Technology Letters, 2014, 26(20): 2055–2057
68. Bradley D J, Bates B, Juulman C O L, Kohno T. Recent developments in the application of the fabry-perot interferometer to space research. Journal de Physique Colloques, 1967, 28 (C2): 280–286
69. Mehra R, Shahani H, Khan A. Mach Zehnder Interferometer and its Applications. IJCA Proceedings on National Seminar on Recent Advances in Wireless Networks and Communications, 2014, NWNC (1): 31–36
70. Van-Pham D, Nguyen M, Nakanishi H, Norisuye T, Tran-Cong-Miyata Q. Applications of Mach-Zehnder interferometry to studies on local deformation of polymers under photocuring. In: Banishev A, Wang J, Bhowmick, eds. Optical Interferometry. London: IntechOpen, 2017, 25–39
71. Markovich R J, Pidgeon C. Introduction to Fourier transform infrared spectroscopy and applications in the pharmaceutical sciences. Pharmaceutical Research, 1991, 8(6): 663–675

Muhammad Noaman Zahid is a doctoral student in the PhD program in School of Optics and Photonics at Beijing Institute of Technology, China. He received his M.S. degree in Electronics Engineering from Muhammad Ali Jinnah University (MAJU), Pakistan, in 2015. His primary area of expertise is RF circuit designing and fabrication for wireless and RFID applications.

Jianliang Jiang received his Ph.D. degree from Beijing Institute of Technology (BIT) in 2005. He had worked as a visiting scholar in Department of Material Science and Engineering, University of Washington, Seattle, USA and Institute of Semiconductor Technology, University of Paderborn, Germany. He is now working at School of Optics and Photonics, BIT. His current research focuses on RFID technology and its applications, novel optoelectronic device and its applications.

Saad RIZVI is currently pursuing his doctorate at Beijing Institute of Technology. His research interests include optical fiber based technologies and quantum optics.